An iterative multiple sampling method for intrusion detection

MWITONDI, Kassim and ZARGARI, Shahrzad <http://orcid.org/0000-0001-6511-7646>

An Iterative Multiple Sampling Method for Intrusion Detection

Kassim S. Mwitondi[1] and Shahrzad A. Zargari[1]

[1]Sheffield Hallam University, Faculty or Arts, Computing, Engineering and Sciences

Abstract

Threats to network security increase with growing volumes and velocity of data across networks, and they present challenges not only to law enforcement agencies, but to businesses, families and individuals. The volume, velocity and veracity of shared data across networks entail accurate and reliable automated tools for filtering out useful from malicious, noisy or irrelevant data. While data mining and machine learning techniques have widely been adopted within the network security community, challenges and gaps in knowledge extraction from data have remained due to insufficient data sources on attacks on which to test the algorithms accuracy and reliability. We propose a data-flow adaptive approach to intrusion detection based on high-dimensional cyber-attacks data. The algorithm repeatedly takes random samples from an inherently bi-modal, high-dimensional dataset of 82332 observations on 25 numeric and two categorical variables. Its main idea is to capture subtle information resulting from reduced data dimension of a large number of **malicious** flows and by iteratively estimating roles played by individual variables in construction of key components. Data visualisation and numerical results provide a clear separation of a set of variables associated with attack types and show that component-dominating parameters are crucial in monitoring future attacks.

Key Words: *Cross-Validation, Cyber-Security, Data Mining, Dimensional Reduction, Intrusion Detection, Principal Component Analysis*

1 Introduction

Anomaly intrusion detection deals with detection of unknown malicious traffic across networks which can be difficult to identify without planned intervention. Network administrators struggle to keep up with Intrusion Detection System (IDS) alerts, and often manually examine system logs to discover potential attacks. In recent years, data mining and machine learning techniques have widely been adopted within the network security community [1, 2] mainly due to the need for a greater understanding of the underlying intrusion detection rules in the Big Data Era [3]. These developments have brought about both opportunities and challenges, requiring novel approaches to security design and modelling [4, 5]. While various tools, methods and techniques have been developed to deal with intrusion detection and ensure network security, gaps remain, apparently due to insufficient data sources on attacks on which to train and test intrusion detection algorithms. We propose a data-flow adaptive approach to intrusion detection based on high-dimensional cyber-attacks data described in Section 3.1. Our approach derives from the original ideas in [6, 7] and [8] who laid down the general framework for domain-partitioning rule-based intrusion detection. In particular, [6] applied association rules and frequent episodes from audit data for feature selection processes while [7] combined association mining with classification. Both were driven by "the degree of confidence" associated with intrusion detection–a parameter that heavily relies on samples, hence a key challenge in knowledge extraction from data. This paper seeks to uncover the general intrusion behaviour via multiple sampling. In particular, the paper focuses on dimensional reduction as discussed in [9, 10, 11] and its main objectives are defined as follows.

1. To uncover natural groupings in data traffic through multiple sampling and validation
2. To comparatively assess the emerging naturally arising groupings and
3. To propose a data-adaptive framework for future network intrusion detection

The paper is organised as follows. Section 2 examines previous work relating to the overall behaviour of intrusion and normal activities. It is followed, in Section 3, by the methods outlining the data sources and the adopted methods.

Data analyses, results and discussions are in Section 4 and concluding remarks and recommendations in Section 5.

2 Background

Data sampling, randomness, multicollinearity, missing data and outliers are some of the main issues which data analysts have to deal with in their quest to attain modelling accuracy and reliability. Many have been widely studied and documented–see, for instance, [12, 13] & [14]. The need for flexible and adaptive security oriented approaches to intrusion detection has triggered a growing interest in computational intelligence methods–artificial neural networks, fuzzy systems, evolutionary computation, artificial immune systems, swarm intelligence and soft computing [1]. Identifying the most relevant features in intrusion detection is not confined to algorithmic computing as it depends much on existing expert domain knowledge skills and the way they are combined with automated tools.

Combining existing domain knowledge and automated learning techniques to solve the intrusion detection problems is generally attributed to the overall objective of data mining, i.e., knowledge extraction from data. Typically, frameworks for attaining that objective are based on pre-defined ontologies with inherently highly dynamic parameters. The dynamics of these parameters are encapsulated within the domains of unsupervised and supervised modelling for which many applications have been developed in recent years [2]. This paper builds upon some of the recent developments and it seeks to develop an integrated strategy to harmonising inherent dynamics in modelling cyber-attacks.

3 Methods

Adopted methods fulfil the following key functions–data understanding, cleansing, clustering and interpretation. More specifically, the paper explores a high-dimensional dataset for systematic characteristics of cyber-attacks. However, capturing and managing the dynamics of cyber-attacks constitute a fundamental challenge, not least because of inherent randomness in data, against the backdrop of which the study motivation and objectives are described.

3.1 Data Sources

Potentially highly correlated data variables were generated from thousands of raw network packets of the UNSW-NB 15 created by the IXIA PerfectStorm tool in the Cyber Range Lab of the Australian Centre for Cyber Security (ACCS). The dataset, created using twelve algorithms [15, 16], represents a high-dimensional data which we denote by

$$\Omega = x_{i,j}[\tau]\ i = 1, 2, 3 \ldots n;\ j = 1, 2, 3, \ldots p;\ 2 \leq \tau \leq n \tag{1}$$

where $n = 82,332$ is the number of observations, $p = 27$ is the number of variables and τ is the sample size randomly selected from Ω, with replacement. The dataset, the attributes of which and summary are shown in Figure 1, represents 37,000 *normal* flows–almost 45% of the total flow, and nine different types of *malicous* flows. Some of the variables on the left hand side (LHS) panel derive from others–e.g., **tcprtt** is the sum of **synack** and **ackdat** and **label** is a binarized version of **attacka**. Apparently, the multivariate data present an ideal case of multicollinearity.

NAME	TYPE	DESCRIPTION
dur	Float	Record total duration
spkts	integer	Source to destination packet count
dpkts	integer	Destination to source packet count
sbytes	Integer	Source to destination transaction bytes
dbytes	Integer	Destination to source transaction bytes
rate	Integer	Transmission rate
sttl	Integer	Source to destination time to live value
dttl	Integer	Destination to source time to live value
sload	Float	Source bits per second
dload	Float	Destination bits per second
sloss	Integer	Source packets retransmitted or dropped
dloss	Integer	Destination packets retransmitted or dropped
sintpkt	Float	Source interpacket arrival time (mSec)
dintpkt	Float	Destination interpacket arrival time (mSec)
sjit	Float	Source jitter (mSec)
djit	Float	Destination jitter (mSec)
swin	Integer	Source TCP window advertisement value
dwin	Integer	Destination TCP window advertisement value
stcpb	Integer	Source TCP base sequence number
dtcpb	Integer	Destination TCP base sequence number
smean	Integer	Source transmitted packet size mean
dmean	Integer	Destination transmitted packet size mean
tcprtt	Float	TCP connection setup round-trip time ('synack' plus 'ackdat').
synack	Float	TCP connection setup time between the SYN and the SYN_ACK packets.
ackdat	Float	TCP connection setup time between the SYN_ACK and the ACK packets.
attacka	Nominal	Attack type
label	Binary	Binarised transmission – normal or attack

	Normal	Attack	Percentage
Analysis	0	677	1.49%
Backdoor	0	583	1.29%
DoS	0	4,089	9.02%
Exploits	0	11,132	24.56%
Fuzzers	0	6,062	13.37%
Generic	0	18,871	41.63%
Normal	37,000	0	0.00%
Reconnaissance	0	3,496	7.71%
Shellcode	0	378	0.83%
Worms	0	44	0.10%

Table 1: Data attributes and class labels (LHS) and summary of the UNSW-NB 15 data flow types (RHS)

The right hand side (RHS) panel exhibits nine *malicious* categories and one *normal*. The former takes two forms–binomial and multinomial–forming a good data source for multiple sampling, training and testing. To fulfil the foregoing objectives, sampled subsets $x_i[\tau]$ where τ is an indicator of sample sizes are extracted for natural grouping.

3.2 Modelling Strategy

The samples are used to form natural groupings $C_{i\tau}$ each with a notional probability $\pi_k[\tau]$ such that $\sum_{k=1}^{K} \pi_k[\tau]$, where $k = 1, 2, \dots K$ is the number of groups and the $p-$dimensional probability function $p\left(x_{\tau,j}, \omega_k\right)$ is fully described by the distributional parameters ω_k. Throughout the samples, one parameter of interest is

$$\xi_\tau = \frac{\sum_{i=1}^{n} \hat{z}_{i,k}[\tau]}{\sum_{i=1}^{n} \hat{z}_{i,k}[\tau] + \sum_{i=1}^{n} \hat{z}_{i,\bar{k}}[\tau]} \propto \sum_{k=1}^{K} \pi_k \tag{2}$$

where $\hat{z}_{i,k}[\tau]$ is an indicator variable denoting membership to group k or otherwise and $\tau = 1, 2, 3 \dots m$ is the sample number. Now, consider a case from a completely random traffic in which $n_a = \sum_{i=1}^{n} \hat{z}_{i,k}[\tau]$ is the total number of cases identified as malicious and $n - n_a = \sum_{i=1}^{n} \left(1 - \hat{z}_{i,k}[\tau]\right)$. Given random sampling, a natural estimator for the average *normal* flow effect can be presented as the difference in the average outcomes of the cases identified as *normal* versus identified as *malicious*. The parameter of interest in Equation 2 leads to the expression in Equation 3.

$$\frac{1}{n} \sum_{i=1}^{n} \left[\frac{\hat{z}_{i,k}[\tau] x_{i,k}[\tau]}{\frac{n_a}{n}} - \frac{\left(1 - \hat{z}_{i,k}\right)[\tau] x_{i,k}[\tau]}{\frac{n - n_a}{n}} \right] \propto \xi_\tau \tag{3}$$

Since every sample is fixed, randomness only manifests in the component $\hat{z}_{i,k}[\tau]$ and subsequently in $\xi_\tau \propto \pi_k$. Thus, the main idea of our strategy is that, by treating membership to these group proportions as missing data and repeatedly sampling and validating clusters, we characterise the overall behaviour of cyber-intrusion. That is, given x_τ as defined above, we can separate k groups with probabilities π_k and $\pi_{\bar{k}}$ corresponding to different descriptions of intrusion. Correlation analysis, Principal Component Analysis (PCA) and Kernel Density Estimation (KDE) are well-known conventional methods that can be applied to analyse the variations in Equation 3. In particular, the KDE, defined as

$$\hat{f}_\beta\left(x_{i\tau}\right) = \frac{1}{\beta} \sum_{i=1}^{n} K_\beta\left(\hat{z}_{i\tau} x - x_{i\tau}\right) = \frac{1}{n\beta} K\left(\frac{\hat{z}_{i\tau} x - x_{i\tau}}{\beta}\right) \tag{4}$$

where $\int K_\beta\left(\hat{z}_{i\tau} x - x_{i\tau}\right) = 1$ is zero-centred and the key parameter $\beta > 0$ determines the number of emerging structures in the sample and therefore its optimal value is proportional to the variations between $\hat{z}_{i,k}$ and $1 - \hat{z}_{i,k}$. Likewise, we can reduce the data dimension by generating *uncorrelated* new variables via PCA whereby each derived components are linear combinations of the original variables and ordered in accordance with variation they account

for. For the $n_\tau \times p$ matrix from each sample, we can compute matrix V which diagonalises the covariance matrix Σ such that $\mathbf{V^{-1}\Sigma V} = \mathbf{G}$, where $\mathbf{G}$ is a matrix of the *eigenvalues* of $\mathbf{\Sigma}$. The columns of $\mathbf{V}$ are *orthorgonal* to each other and they define the principal components whereas the diagonal values of $\mathbf{G}$ are the variances of the components. The orthogonal $\mathbf{V}$ are the *eigenvectors*, i.e., uncorrelated data with directions and magnitude defining each component.

As far as optimising variation in data is concerned, β and *eigenvalues* play a similar role and so, in both cases, we can optimise their expected values via repeated sampling. For example, through each sample we can generate a correlation matrix that is re-ordered based on the angular order of the eigenvectors as defined in Equation 5.

$$\rho_{i,\tau} = \begin{cases} \tan\left(\frac{e_{i,2}}{e_{i,1}}\right), & \text{if} \quad e_{i,1} > 0 \\ \tan\left(\frac{e_{i,2}}{e_{i,1}}\right) + \pi, & \text{if} \quad e_{i,1} < 0 \end{cases} \tag{5}$$

where e_1 and e_2 are the largest *eigenvalues* from the matrix. The mechanics for implementing the foregoing strategy in pursuit of the objectives outlined in Section 1 are presented in a finite number of steps in Algorithm 1.

Algorithm 1

procedure OPTIMAL VARIATION(OPTIVA)
  Load $x_{i,j} \subset \Omega$.
  Set: $\mathcal{S}[\tau] = s_1, s_2, \ldots s_m$ (Sample sizes vector of length m) .
  Init: $\Phi_\rho(.) = \emptyset$ (Correlation Storage Matrix) .
  Init: $\mathcal{L}(.) = \emptyset$ (Loadings/Directions Storage Matrix) .
  Init: $\Delta\mathcal{L}(.) = \emptyset$ (Sample-based Variations in Loadings/Directions) .
  while $\mu \leq m$ **do**
    Update $\mu := \mu + 1$.
    $\mathcal{S}_\tau \leftarrow \hat{z}_{i,j} x_{i,j}[\tau] \subset \Omega$.
    Update $\Phi_\tau(.) \leftarrow \rho_{i,\tau} \leftarrow \mathcal{S}_\tau$.
    Update $\mathcal{L}_\tau(.) \leftarrow \left\{ v_{j,\tau};\ g_{j,\tau};\ \frac{d_{j,\tau}}{\sum_{i=1}^{n} d_{i,\tau}} \right\} \leftarrow \mathcal{C}_{i,j}[\tau]$.
    Update $\Delta\mathcal{L}(.) \leftarrow \overset{+}{-} \{\mathcal{L}_\mu - \mathcal{L}_{\mu+1}\}$.
    for $\eta = 1 \rightarrow \dim \mathcal{L}_{i,j}$ **do**
      $\mathcal{CA}_{\Delta,\tau} = \frac{\sum_{\iota=1}^{\mu} \Delta\mathcal{L}(.)}{\mu} \iff \frac{\Delta\mathcal{L}_{\mu+1}(.) + \mu\mathcal{CA}_{\Delta,\mu}}{\mu+1} = \mathcal{CA}_{\Delta,\mu+1}$ (Cummulative Moving Average) .
      Plot $\mathcal{CA}_{\Delta,\mu+1}[j,\tau]$ (For Validation) .
      Store $\mathcal{CA}_{\Delta,\mu+1}[j,\tau]$.
      Store $\mathcal{L}_\mu$ (Dom) $\leftarrow \mathcal{CA}_{\Delta,\mu+1}[j,\tau]$ (Dominant Loadings) .
    end for
  end while
  Output and interpret $\mathcal{C}_{m,i,j}[\tau]$.
end procedure

The algorithm repeatedly takes up to m samples of different sizes, spacing and order from Ω. The magnitudes can be determined via exploratory analyses but the order is not particularly important. The algorithm's main idea is to compare variations in rotations - the quantities which form the principal components. Averaging of the variations may be confined to a few components contributing to the highest variation in data or may include all $j = p$ components.

4 Results and Discussions

In this section we present key results from implementing Algorithm 1 on data repeatedly sampled from Ω, as defined in Equation 1 and described in Table 1. As noted above, some of its key inputs such as sample sizes and spacing can be determined via exploratory analysis for insights into variable correlations, emerging natural structures and validation.

4.1 Preliminary Analyses

The two panels in Figure 1 exhibit correlation structures among the transmission variables. They both provide insights into how different transmission parameters interact based on which we can adjust the sampling parameters mentioned above. The RHS panel provides an ordered visual pattern that can be useful further analyses as in PCA below. Figure 1

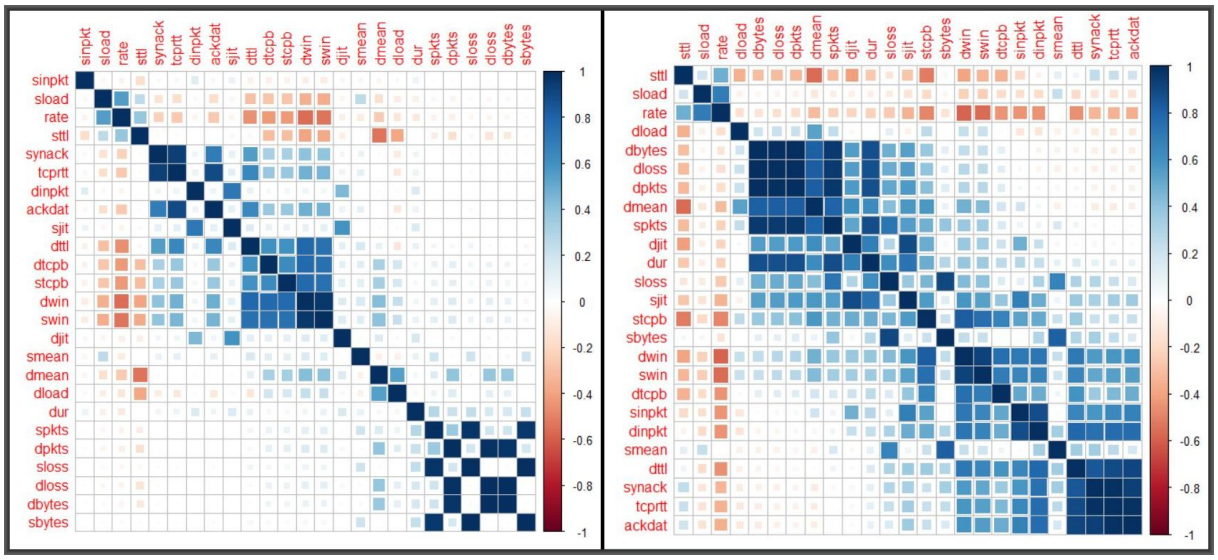

Figure 1: Full data correlogram (LHS) and one for sample size 50 (RHS)

exhibits two extreme cases of the variable correlations based on the number of observations. In both cases it is evident that the variables **dpkts, dloss** and **dbytes** are highly correlated–almost perfectly positive. The same can be said of **synack** and **tcprtt**; **tcprtt** and **ackdat** as well as **spkts, sloss, sbytes**. While there aren't many extreme cases of high correlation in the full dataset, samples drawn from it indicate high multicollinearity among the variables. Interpretation of principal components, discussed below, is preceded by computations of correlations between the original data for each variable and each extracted component. It is worth noting that interpretation of the principal components is based on finding the variables which most correlate with the components, as discussed below.

4.2 Extracting, Interpreting and Optimising Principal Components

The panels in Figure 2 represent the same plot of the first two components from the full data labelled by all type of data flows on the left and by the binarised flow on the right. By the **eigenvalue rule** we can accept 8 components which have a value greater than 1. The first eight components account for 81.34% of variation in the original data with the first through eighth accounting for 24.3%, 14.4%, 11.55%, 8.97%, 8.48%, 5.15%, 4.28% and 4.19% respectively. We see, on the left hand side panel, that there is a clear separation of attributes that describe **Exploits**, **Dos** and **Generic** attack types–exhibited on the right as **malicious** and **normal** flows. That is, the first component strongly correlates with these variables as well as with normal flow–increasing with **malicious** and decreasing with **normal** flows. This suggests that the three attack types vary together–i.e., as one goes up the other two tend to do the same. We can use the numerics associated with this component to measure and monitor the risk of these type of attacks.

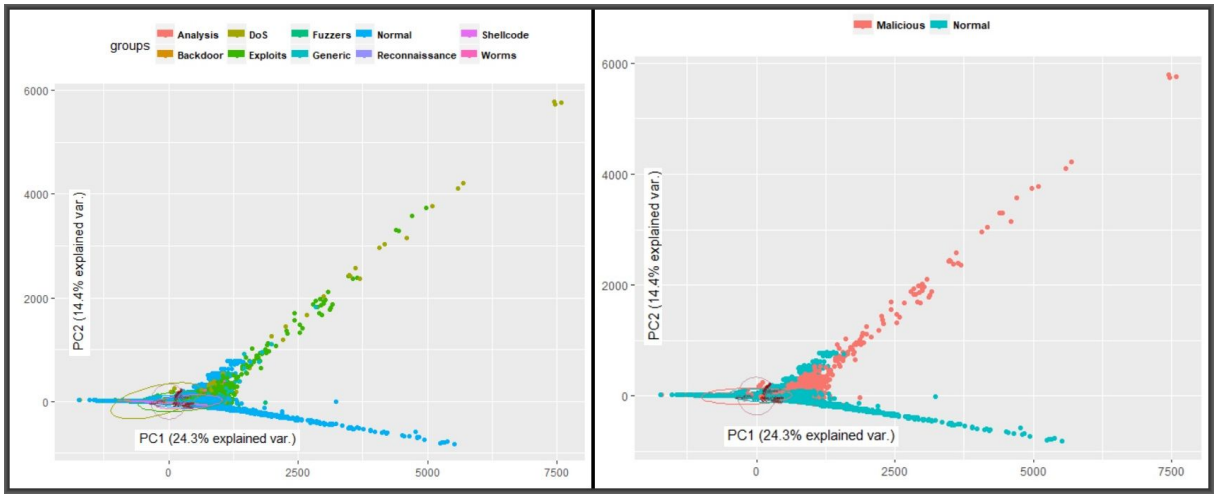

Figure 2: Two panels of the same plot with multi-class and binary labelling

Loadings of the first eight components from the full data are presented in Table 2, where it can be seen that there is no single very high correlation between the variables and the extracted components. The magnitudes and directions of the loadings underline the existing multicollinearity among the data flow variables which can also be explained by the large number of components extracted. These metrics represent the influence of the individual variables in constructing the component and, hence, by repeatedly sampling and extracting new components we generate a range of new metrics which can be aggregared and averaged in line with Algorithm 1.

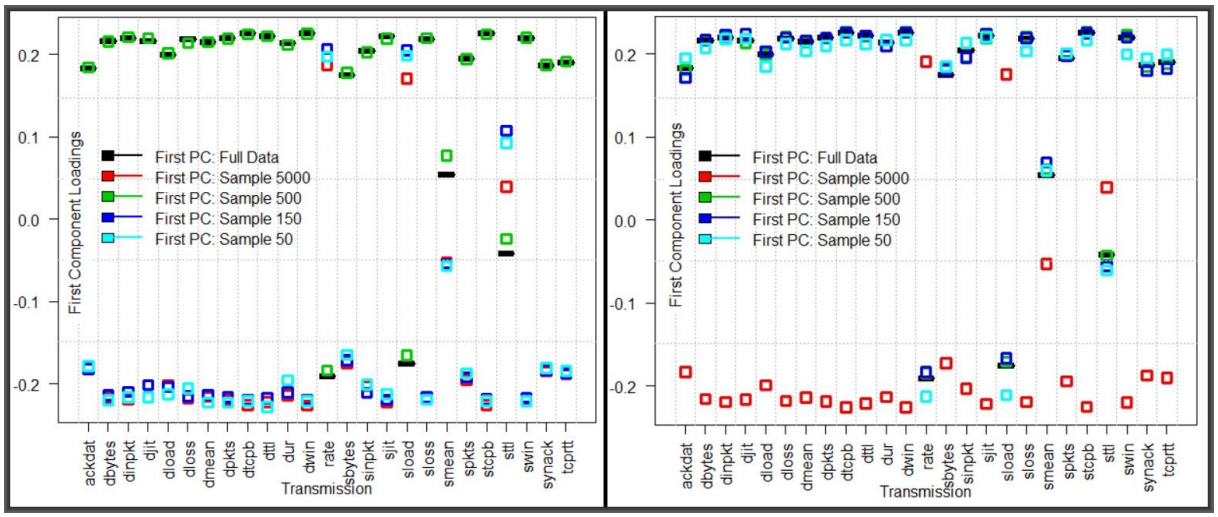

Figure 3: Selected runs for first component patterns generated by the full data and different sample sizes

Particularly interesting are the variables which contribute to the highest variation in the data–these are the ones which are most highly correlate with extracted components. The two panels in Figure 3 show patterns generated by the full data and four different sample sizes. In both cases, the full dataset exhibits a predominantly positive contribution by most variables in forming the cluster but samples, large and small, exhibit both positive and negative relationships between the variables and the component exhibiting, in both cases, a clear binary pattern.

LOADINGS FOR THE FIRST EIGHT COMPONENTS - FULL DATA								
Variable	**PC1**	**PC2**	**PC3**	**PC4**	**PC5**	**PC6**	**PC7**	**PC8**
dur	0.214	0.127	0.020	-0.112	0.210	-0.374	0.196	0.026
spkts	0.194	-0.275	0.094	-0.041	0.333	-0.138	0.335	-0.436
dpkts	0.219	-0.181	-0.045	0.104	-0.206	-0.100	0.070	-0.035
sbytes	0.174	-0.288	0.248	-0.355	0.120	-0.064	0.163	-0.236
dbytes	0.216	-0.200	-0.065	0.123	-0.219	-0.105	0.073	-0.028
rate	-0.191	-0.195	0.290	0.267	-0.034	0.142	-0.083	-0.142
sttl	-0.042	0.196	0.628	0.297	0.074	-0.438	0.118	0.290
dttl	0.221	-0.033	-0.018	0.088	-0.341	-0.081	0.091	0.111
sload	-0.177	-0.199	0.410	0.168	-0.053	0.100	-0.080	-0.050
dload	0.200	-0.257	-0.102	0.151	-0.350	-0.105	0.134	0.116
sloss	0.218	-0.087	0.071	0.046	0.239	0.225	0.073	0.219
dloss	0.218	-0.149	0.032	0.115	0.170	0.226	0.011	-0.123
sinpkt	0.204	0.192	-0.176	-0.203	0.183	-0.147	-0.051	0.143
dinpkt	0.219	0.062	0.037	0.057	-0.047	-0.222	-0.527	-0.155
sjit	0.221	0.110	0.009	-0.055	0.141	-0.158	-0.036	0.262
djit	0.216	-0.021	0.024	0.102	0.092	-0.210	-0.593	-0.283
swin	0.219	-0.025	0.049	0.100	0.207	0.240	0.001	0.379
stcpb	0.225	-0.041	0.058	0.094	0.092	0.236	-0.100	0.089
dtcpb	0.225	-0.041	0.058	0.094	0.091	0.235	-0.100	0.087
dwin	0.226	-0.041	0.058	0.094	0.092	0.233	-0.100	0.084
tcprtt	0.190	0.366	0.144	0.000	-0.168	0.176	0.109	-0.209
synack	0.186	0.373	0.143	-0.004	-0.172	0.184	0.138	-0.206
ackdat	0.183	0.390	0.148	-0.008	-0.186	0.159	0.107	-0.239
smean	0.054	-0.168	0.380	-0.700	-0.292	0.090	-0.204	0.213
dmean	0.214	-0.166	-0.077	0.124	-0.310	-0.115	0.081	0.085

Table 2: Loadings of the first eight components accounting for 81.34% of the variation in the original data

We can take a closer look at the structure of the components–particularly how its numerics can be used to measure and monitor attack risks. The **prcomp** in **R** returns a matrix of **loadings**, the columns of which contain the eigenvectors. Since each sample yields a different set of these values which occur in a subspace of the retained components and, as such, they are affected by the choice of the subspace. It is therefore reasonable to consider their descriptive statistics over different sample space sizes in order to attain robust interpretation of their role in forming the components. Key descriptive statistics taken from across 40 random samples for each of the 25 malicious flows are presented in Table 3 with a graphical illustration in Figure 4. Note that most of the variables average above zero and only a handful–**rate, stll, sload** and **sinpkt** take a below zero average which is in line with the upward trend in PC1 in Figure 2.

Variable	Mean	STD	Minimum	Maximum	Median
dur	0.053241072	0.049069703	-0.089779978	0.096179555	0.070608542
spkts	0.079086356	0.073230517	-0.131049938	0.190921677	0.099165296
dpkts	0.095680718	0.092280686	-0.176525333	0.185144282	0.115784116
sbytes	0.048757831	0.044907203	-0.07860671	0.104355861	0.061818932
dbytes	0.073949495	0.07073006	-0.128000773	0.140550935	0.090410086
rate	-0.18776741	0.168431339	-0.25667896	0.257028067	-0.250259704
sttl	-0.12149291	0.111207664	-0.180892452	0.173475353	-0.161471934
dttl	0.241772537	0.214230803	-0.328501048	0.331045934	0.322263355
sload	-0.130025648	0.119130268	-0.190388137	0.193535459	-0.174953137
dload	0.058215931	0.05468673	-0.092486021	0.097995809	0.076081787
sloss	0.057920965	0.053260196	-0.088886221	0.13589708	0.071644141
dloss	0.081481929	0.07847966	-0.144333769	0.161010325	0.098331803
sinpkt	-0.018169	0.015626402	-0.034045938	0.025287213	-0.023316505
dinpkt	0.041195128	0.038584336	-0.070708227	0.092707723	0.054827379
sjit	0.055623151	0.050451569	-0.081847812	0.083059598	0.073129513
djit	0.068081149	0.068293189	-0.113622275	0.118902853	0.090858174
swin	0.269965189	0.241070194	-0.3643555	0.367607174	0.360468887
stcpb	0.230637173	0.206154129	-0.311387749	0.314365753	0.308433324
dtcpb	0.231057451	0.205850281	-0.312207439	0.314568604	0.308076007
dwin	0.277203906	0.247573503	-0.374630352	0.377052807	0.36994129
tcprtt	0.199757556	0.174533831	-0.270697064	0.286146344	0.26590308
synack	0.177062695	0.154497947	-0.245453323	0.268009645	0.234418956
ackdat	0.193011274	0.171012144	-0.266092244	0.273382985	0.258014823
smean	0.04823361	0.042484211	-0.068058027	0.079574215	0.063744348
dmean	0.13739165	0.126189404	-0.207957301	0.218783984	0.178772078

Table 3: Descriptive statistics of each of the 25 component forming variables across 40 samples

The parameters used in constructing Table 3 and Figure 4 are proportional to the coefficients of the linear combination of the original variables in Table 1. The linear combination makes up PC1 and, in this particular application, they impinge on the nature of the traffic and so they can be used as predictors of the phenomenon that they symbolise. The degree of influence of each variable in constructing the components can be deduced from both Tables 2 and 3 as well as from Figure 4. As implied by Equation 3, randomness manifests in sampling and, hence, in the calculation of $\xi_\tau \propto \pi_k$ and it is in this sense that repeated sampling characterises the overall behaviour of cyber-intrusion.

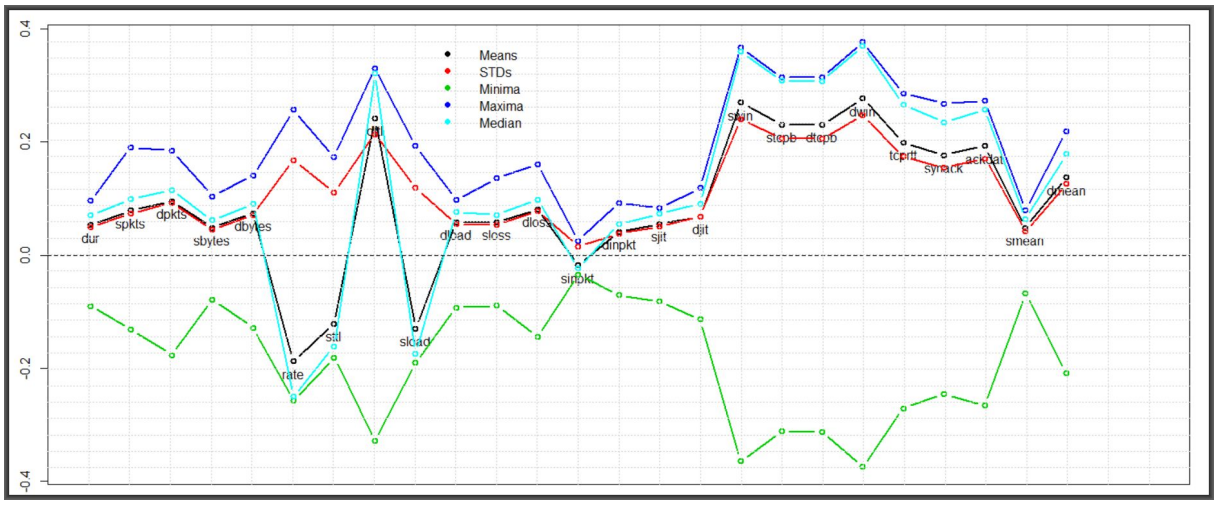

Figure 4: A graphical illustrations of the malicious flows descriptive statistics in Table 3 from across 40 samples

Both the original full data and repeated samples exhibit a clear pattern of duality. The left hand side panel in Figure 5 shows the densities of the full data and three random samples of sizes 50, 500 and 5000 while the patterns on the right are proportional to the correlations between the individual variables and the first component across 40 samples.

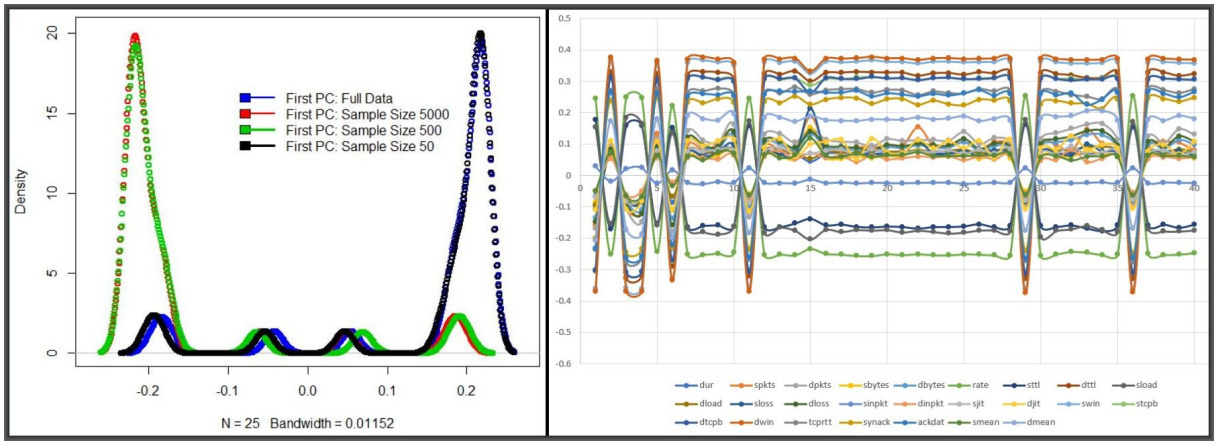

Figure 5: Component one densities from selected samples and 40 samples variable correlations with the component

The fact that no single variable exhibits significantly high correlation with the component in the right hand side panel of Figure 5 highlights the potential masking of the flows. However, the fact that together the variables show a consistent separation of the data into two distinctive regions, with several variables such as **dttl, sttl, dload, rate, dloss** etc, standing out, implies that based on patterns and relationships from both the full data and multiple samples drawn from it–i.e., given x_τ as defined in Section 3.1, we can separate k groups with probabilities π_k and $\pi_{\bar{k}}$ corresponding to different descriptions of intrusion. More specifically, we can use historical data numerics associated with the first significant components, say, to train and test models to measuring and monitoring the risk of known types of intrusion.

5 Concluding Remarks

We have presented a data-flow adaptive method for intrusion detection based on repeated sampling from a high-dimensional cyber-attack data source. We set off to achieve the three objectives in Section 1 from the premises of

the two well-documented intrusion detection techniques - **misuse** in [17] and **anomaly** detection [18]. Our modelling interpretation of the former is that of rule-based decision that would help identify a suspicious behavior by comparing it to known catalogued malicious flows. On the other hand, the latter, as in many applications, was perceived as a model, the departure from which is a cause for alarm. We took a unified approach to the two and in both cases the binary and multi-class labels in the dataset used in the study provided the basis for such an approach. Comparing the performance of our method of choice, PCA, with other dimensional reduction techniques would have been ideal, but for the limitations imposed by the study objectives. However, we were able to demonstrate, via Algorithm 1, how information resulting from reduced data dimension of a large number of **malicious** flows, can be utilised to monitor the emerging structures and potentially be used as inputs in build robust intrusion detection systems. The results were achieved via repeated sampling, yielding parameters that were generally used to fine-tune potential structures in each sample. Aggregating the parameters over many runs, we were able to reproduce consistent patterns of the data duality. The resulting patterns render themselves readily to predictive modelling using the two class labels and therefore provide scope for extension into identifying new attacks. For that to happen, however, data attributes must always be added to the training and testing set repositories, not least because of the dynamic nature of intrusion.

Novelty of our approach derives from iterative estimation of the roles played by individual variables in construction of components, particularly the potential for monitoring future attacks by focusing on the metrics that dominate the components. Without being influenced by the provided levels of attack types, our findings are particularly intriguing for two reasons–the duality may mean either masking or swamping of attack types. That is, some currently unknown attack types may slip through as **normal** which is why it is imperative to highlight two important aspects of this study–the mechanics of the algorithm and the data attributes. If we knew the relevant density functions and classes of attack, we would simply observe data flows and make predictions. But in practice we have to estimate these parameters from random data and test our algorithms on another random dataset. Our contribution focused on variability as determined by $z_i[\tau]$ and proportions π_k. For continuous attributes, these parameters typically derive from the mean and covariance matrices of the normal mixtures while for categorical data, they are group proportions. Finally, our choice of the angular order of the eigenvectors was justified by the adopted dimensional-reduction methods used as it would make multiple comparisons to be made using other eigenvalues. There are other ways of re-ordering the correlation matrix to help visualisation of the inherent patterns. This random nature of analytical studies stipulates that research be a function of data sharing, design, experimental setups and research findings. One way of achieving that goals is to go the way of open source repositories. We expect that this paper will contribute towards that aspiration, attain data enrichment, methods enhancements and open new paths to future studies.

References

[1] S. Wu and W. Banzhaf. The use of computational intelligence in intrusion detection systems: A review. *Applied Soft Computing*, 10(1):1–35, 2001.

[2] R. Sommer and V. Paxson. Outside the closed world: On using machine learning for network intrusion detection. *IEEE Symposium on Security and Privacy*, 2010.

[3] S. Suthaharan. Big data classification: Problems and challenges in network intrusion prediction with machine learning. *SIGMETRICS Perform. Eval. Rev.*, 41(4):70–73, April 2014.

[4] Y. Demchenko, C. Ngo, C. de Laat, P. Membrey, and D. Gordijenko. Big security for big data: Addressing security challenges for the big data infrastructure. In *Secure Data Management*, pages 76 – 94. Springer International Publishing, 2014.

[5] L. Kaufman. Can public-cloud security meet its unique challenges? *IEEE Security & Privacy*, 8:55–57, 2010.

[6] W. Lee, S. Stolfo, and K. Mok. Adaptive intrusion detection: A data mining approach. *Artificial Intelligence Review*, 14:533 – 567, 2000.

[7] S. Noel, D. Wijesekera, and C. Youman. Modern intrusion detection, data mining, and degrees of attack guilt. *Applications of Data Mining in Computer Security: Advances in Information Security*, 6:1–31, 2002.

[8] R. Mitchell and I-R. Chen. Behavior rule specification-based intrusion detection for safety critical medical cyber physical systems. *IEEE Transactions on Dependable and Secure Computing*, 12:16–30, 2015.

[9] M. Maechler, P. Rousseeuw, A. Struyf, M. Hubert, and K. Hornik. *cluster: Cluster Analysis Basics and Extensions*, 2013. R package version 3.4.0.

[10] K. V. Mardia, J. T. Kent Kent, and J. M. Bibby. *Multivariate Analysis*. Academic Press, 1979.

[11] N. Kambhatla and T. Leen. Dimension reduction by local principal component analysis. *Neural Computation*, 9:1493–1516, 1997.

[12] K. Mwitondi, C. Taylor, and J. Kent. Using boosting in classification. *Proceedings of the Leeds Annual Statistical Research (LASR) Conference; Leeds University Press*, pages 125–128, 2002.

[13] K. Mwitondi, R. Moustafa, and A. Hadi. A data-driven method for selecting optimal models based on graphical visualisation of differences in sequentially fitted roc model parameters. *Data Science*, 12:WDS247–WDS253, 2013.

[14] K. Mwitondi and R. Said. A data-based method for harmonising heterogeneous data modelling techniques across data mining applications. *Statistics Applications and Probability*, Pro 2(3):293–305, 2013.

[15] N. Moustafa and J. Slay. Unsw-nb15: A comprehensive data set for network intrusion detection systems. *Cyber Range Lab of the Australian Centre for Cyber Security (ACCS)*, 2015.

[16] N. Moustafa and J. Slay. The evaluation of network anomaly detection systems: Statistical analysis of the unsw-nb15 data set and the comparison with the kdd99 data set. *Security Journal: A Global Perspective*, pages 1–14, 2016.

[17] S. Kumar and E. Spafford. A software architecture to support misuse intrusion detection. *Proceedings of the 18th National Information Security Conference*, pages 194–204, 1995.

[18] P. A. Porras and P. G. Neumann. Event monitoring enabling responses to anomalous live disturbances. *Proceedings of National Information Systems Security Conference, Baltimore MD*, 1997.